(ANPA Conference 2023)
ISSN: 2392-473X(Print), 2738-9537 (Online)

Research Article ©Nepal Physical Society
DOI:http://doi.org/10.3126/jnphyssoc.v9i3.62451

Nickel-Doped Tungsten Disulfide for Energy Storage Applications

Keshab Pandey[1, a)] and Hae Kyung Jeong[1, 2, b)]

[1)] *Department of Physics, Daegu University, Gyeongsan 38453, Republic of Korea*
[2)] *Department of Energy System Engineering, Daegu University, Gyeongsan 38453, Republic of Korea*

[a)] *Keshab Pandey: keshavpandey48@gmail.com*
[b)] *Hae Kyung Jeong: outron@gmail.com*

Abstract. Nickel-doped hexagonal pyramid-like tungsten disulfide (WS_2) has been synthesized via a simple hydrothermal synthesis method and offers great promise for use in electrochemical energy storage devices such as supercapacitors. The nickel concentration of 3, 4.5, and 6 at. % was added to WS_2. Three-electrode and two-electrode configurations are used to test the electrochemical performances of the materials as prepared. The nickel doping of 4.5 at. % exhibits a high specific capacitance of 144 F g^{-1} at a current density of 1 A g^{-1} with an energy density of 13.3 Wh kg^{-1} and power density of 802 W kg^{-1} for the symmetric supercapacitor device. Increased electrochemically active surface area and decreased impedance are attributed to the improved supercapacitive performances. Finally, high specific power retention (92.1%) and Coulomb efficiency (86.0%) were demonstrated after 3,000 cycles. These results demonstrate that the synthesized nickel-doped WS_2 can be used for high-performance supercapacitor flexible electrodes.

Received: 31 August, 2023; **Revised**: 21 December, 2023; **Accepted**: 21 December, 2023

Keywords: Tungsten disulfide; nickel doping; supercapacitor

1. INTRODUCTION

Recent advancements in electrochemical energy storage technologies have captured the attention of researchers, primarily driven by concerns over the energy crisis and ecological degradation. Among these technologies, supercapacitors (SCs) have garnered significant focus due to their exceptional attributes, such as rapid charging and discharging capabilities, prolonged lifespan, robust safety profile, and minimal ecological impact [1-5]. Nonetheless, the swift evolution of electronic devices has highlighted the limitation of supercapacitors (SCs) in terms of their relatively modest energy density, which poses challenges to their effective utilization [6-8]. In this context, the imperative lies in the identification of appropriate components, particularly structured electrode materials, that can effectively enhance the performance of SCs.

Tungsten disulfide (WS_2), a representative example of layered transition-metal dichalcogenides (TMDs), has recently attracted interest as a prospective electrode material for supercapacitors (SCs) due to its distinctive layered configuration and favorable conductivity properties [9,10]. Numerous approaches, encompassing metal sulfides [10,11], metal oxides [12], and metal carbides [13], have recently emerged to achieve remarkably effective electrodes for supercapacitors. The active sulfur atoms located on the edges have prompted a substantial investigation into transition metal dichalcogenides (TMDs) derived from Group VI elements [14], as potential electrodes with superior efficiency for supercapacitors. Nevertheless, up to the present point, the current WS_2 electrode materials continue to encounter issues in their electrochemical performance.

The incorporation of dopants and impurities into WS_2 and similar transition metal dichalcogenides (TMDs) to alter their characteristics has garnered significant attention [14]. Due to the high electrical resistivity of WS_2, which makes it less suitable for electrochemical devices, the introduction of dopants plays a crucial role in significantly enhancing the electrical conductivity of both WS_2 and other TMDs. Metal doping such as Ni, Co, and Fe to WS_2 electrode materials offers the potential to overcome their inherent limitations, enhancing conductivity, ion diffusion, redox activity, and overall electrochemical performance [15-17]. Nickel (Ni) enables electron transfer from Ni to W because of its lower electronegativity compared

to W. This electron transfer can lead to more efficient and versatile supercapacitors for various applications, primarily by augmenting the presence of active edges [15]. The process of infusing dopants into WS_2 and other TMDs serves the purpose of adjusting the dopant's concentration and type for electronic applications, and these dopants can even induce alterations in the crystal structure [18]. Nonetheless, research into metal doping to WS_2 electrode materials has been limited. For a more thorough understanding, more study in this area is required.

In this study, we synthesized nickel-doped pyramid-like hexagonal tungsten disulfide supercapacitor electrodes by a simple hydrothermal method and the Ni content of 4.5 at. % in WS_2 shows the best electrochemical performance such as a specific capacity of 144 F g^{-1} with an energy density of 13.3 Wh kg^{-1} and power density of 802 W kg^{-1} at a current density of 1 A g^{-1}. Improved supercapacitor efficiency can be achieved with appropriate Ni content in WS_2, attributable to low charge transfer resistance and high electrochemical surface area.

2. Experimental

2.1 Materials

Sodium tungstate dihydrate (Na_2 WO_4. $2H_2O$, $\geq$99%), thiourea (CH_4N_2S, $\geq$99%), cetyltrimethylammonium bromide (CTAB, $\geq$98%), nickel(II) nitrate hexahydrate

($Ni(NO_3)_2.6H_2O$, 99.99%, trace metal basis), hydroxylamine hydrochloride (NH_2OH. HCl, 99%), polyvinyl alcohol (PVA, 99%, hydrolyzed), sulfuric acid (H_2SO_4, $\geq$ 98%), and potassium hydroxide (KOH, $\geq$85%) were obtained from Merck. Ethanol was purchased from Samchun Pure Chemical Co., Ltd. (Seoul, Republic of Korea). A carbon cloth (CC, HCP331, thickness 0.35 mm) was obtained from Wizmac Co., Ltd., Korea.

2.2 Sample preparation

Tungsten disulfide was synthesized using Na_2WO_4. $2H_2O$ (3.3 gm), CH_4N_2S (3.06 gm), NH_2OH. HCl (0.7 gm), doped WS_2, in which nickel(II) nitrate hexahydrate 0.5 gm, 1 gm, and 1.5 gm were added to the powder as a source of nickel, and the end products are named Ni-W-1, Ni-W-2, and Ni-W-3, respectively, the Ni content was controlled.

2.3 Physiochemical characterization

The surface properties and structural attributes were examined using a field emission scanning electron microscope (FESEM) from Hitachi in Japan. In addition, the JEOL S-4300 energy-dispersive X-ray spectroscopy (EDS) apparatus was used to map, configure, and determine the elemental composition of the synthesized samples.

2.4 Preparation of supercapacitor electrodes and gel electrolyte

The commercial carbon cloth (CC) was rectangularly cut to a size of 3 x 1 cm, washed with an HCl solution of 3 mol/L by ultrasonic cleaning for 5 min, and then washed again for 10 min each with DI water and ethanol. This was done to remove any remaining residue from the surface. Finally, the CC strips were dried in a vacuum oven at 65 °C for 12 h and placed in a desiccator before use.

Supercapacitor electrodes and slurry preparation were as follows: 40 ml of DI water were combined with 200 mg of Ni-W-1, 25 mg of CB, and 25 mg of PTFE. The produced solution was then vacuum filtered, dried in an oven at 65 °C for 12 h, and then magnetically agitated for 30 min to create a homogenous dispersion. The 100 mg as-prepared sample was then thoroughly mixed with 10 ml of isopropyl alcohol using magnetic stirring for 1 hour to create the slurry. Then, using a spin coating method (SPIN-1200D, Midas Systems Co., Ltd. Daejeon, South Korea) at 4000 rpm for 1 h, the produced slurry was cast on the CC strips. The prepared supercapacitor electrode was vacuum-dried overnight at 60 °C. The weight difference before and after the deposition was used to carefully estimate the sample's loading amount onto the CC strips. The loaded amount was 1.44 and 1.65 mg cm^{-2} for the Ni-W electrode. The symmetric supercapacitor had two Ni-W electrodes for both the positive and negative electrodes. The separator was constructed using the Whatman cellulose membrane. The resulting supercapacitor device was given the name Ni-W device. The PVA-based gel electrolyte was created by dissolving 6 gm of PVA in 54 ml of DI water at 90 °C and stirring the mixture magnetically until it was clear. After stirring for 10 min, 6 ml of DI water and 6 gm of KOH were added. After 10 min of mixing both solutions at 90 °C while using magnetic stirring, the PVA-based gel electrolyte was ultimately produced.

2.5 Electrochemical characterization

Using (Bio-Logic, SP-150, France), the electrochemical performance of the samples was evaluated at room temperature. Ag/AgCl (3M KCl saturated) was used as the reference electrode while platinum wire worked as the counter electrode in the 6.0 M KOH electrolyte. The

functioning electrodes are as follows: To create a homogeneous mixture, 5 mg of each sample was dissolved in 2 ml of (isopropyl alcohol) IPA using a sonicator. Then, 5 microliters of the sonicated homogeneous solution were used to disseminate the glassy carbon electrode (OD: 6 mm, ID: 3 mm). Working electrodes had a loaded active mass of 2.5 gm/m^2. Using cyclic voltammetry (CV), chronocoulometry (CC), and electrochemical impedance spectroscopy (EIS), materials were electrochemically analyzed. To investigate capacitive behavior and evaluate the reversibility of an electrochemical reaction of the samples, CV measurements were carried out within a potential range of 0 to 0.8 V at scan rates of 10, 25, 50, 100, and 200 mV s^{-1}. As previously mentioned [5,7], CC was utilized to calculate the electrochemically active surface area. Electrochemical impedance spectroscopy (EIS) was utilized to analyze electrochemical impedance performances and characterize electron transfer and recombination processes in the frequency range of 100 MHz to 500 kHz [4,7]. The internal resistance (R_s) and charge-transfer resistance (R_{CT}) might be determined using Z-fitting software based on the analogous Randle circuit utilizing a Nyquist plot (-Im |Z| as a function of Re |Z|). The semicircle diameter represents the charge-transfer resistance.

The cyclic voltammetry (CV), chronocoulometry (CC), and electrochemical impedance spectroscopy (EIS) measures were investigated using two- and three-electrode setups. The CV curve was used to compute the specific capacity (C_s) at F g^{-1} using the following formula [4,5]:

$$C_s = \frac{A}{2XmX\Delta VXv} \quad (1)$$

where A is the integral area under the CV curve in square meters, m denotes the electrode mass, ΔV denotes the potential window in voltage units, and v denotes the scan rate in millivolts per second. The related specific capacitances (Cs), specific energy (E) measured in watt-hours per kilogram (Wh kg^{-1}), specific power (P) measured in watts per kilogram (W kg^{-1}), and coulombic efficiency were calculated using the formulae below. The GCPL discharge curves provided the foundation for these computations [4,5,7]. The discharge time (Δt) measured in seconds and the discharge current (I) measured in amperes are the variables used in the equations.

$$C_s = \frac{IX\Delta t}{mX\Delta V} \quad (2)$$

$$E = \frac{C_sX(\Delta V)^2}{2X3.6} \quad (3)$$

$$P = \frac{EX3600}{\Delta t} \quad (4)$$

$$\text{Coulombic efficiency}\% = \frac{\text{discharge time}}{\text{charge time}} \text{ x } 100\% \quad (5)$$

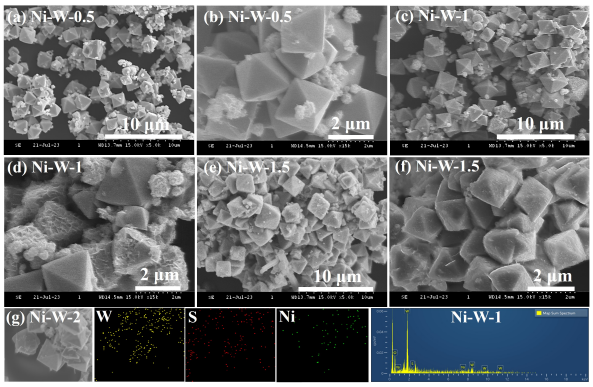

FIGURE 1. SEM images of (a-b) Ni-W-0.5, (c-d) Ni-W-1, and (e-f) Ni-W-1.5 with (g) EDS mapping of Ni-W-2.

3. Results and discussion

Figure 1 shows the SEM images of Ni-W-0.5, Ni-W-1, and Ni-W-1.5. The Ni-W-0.5, doped sample with a nickel content of 0.5 g to WS_2 has a smooth pyramid-type, bulky, and tightly stacked together structure, as seen in Figure 1(a-b), whereas the Ni-W-1, with a nickel content of 1.0 g to WS_2 (Figure 1(c-d)), has a rough surface which may offer many additional active edge sites, partially exfoliated layers, and promotes the high surface area, likely due to the presence of Ni dopants. Furthermore, When the nickel content was increased to 1.5 g, a rough-like structure collapsed and agglomerated particles, as shown in Figure 1 (e-f). Figure 1(g) shows the EDS mapping and elemental composition of Ni-W-1 confirming that nickel-doped WS_2 consists of tungsten, sulfur, and nickel. Detailed elemental information obtained from the EDS results is shown in Table I, which is another evidence of nickel doping. The nickel of 3, 4.5, and 6 at.% was doped into Ni-W-0.5, Ni-W-1, and Ni-W-1.5, respectively.

The scan rate-dependent cyclic voltammetry (CV) results of Ni-W-0.5, Ni-W-1, and Ni-W-1.5 exhibit quasi-rectangular-shaped CV curves at various scan rates from 10 to 200 mV s^{-1} as shown in Figure 2(a-c). The Ni-W-1 sample in Figure 2(b) showed high-rate capabilities, though, with a rectangular form and a significant integrated area. Consequently, compared to the other samples, Ni-W-1 might show a stronger current response. This difference would indicate that Ni-W-1 has distinguishing qualities including a large specific surface area, improved electrical conductivity, and increased capacitance.Using the CV data, Equation (1) could be used to compute the specific capacitance (Cs), which is proportional to the integrated area [5,7]. At a scan rate of 50 mV s^{-1}, Ni-W-1 had the highest capacitance of 148 F g^{-1}. The capacitances of Ni-W-0.5 and Ni-W-1.5 were also found to be 84 and 112 F g^{-1} at the scan rate of 50

TABLE I. Comparison of the elemental distribution of the samples from EDS.

Sample	Element	wt.%	at.%
Ni-W-0.5	W	56.0	11.0
	S	18.0	22.0
	C	14.0	50.0
	O	5.0	14.0
	Ni	3.5	3.0
Ni-W-1	W	53.0	10.0
	S	17.0	19.0
	C	15.0	46.0
	O	9.0	20.5
	Ni	6.0	4.5
Ni-W-1.5	W	52.0	9.0
	S	16.0	18.0
	C	14.0	44.0
	O	10.0	23.0
	Ni	8.0	6.0

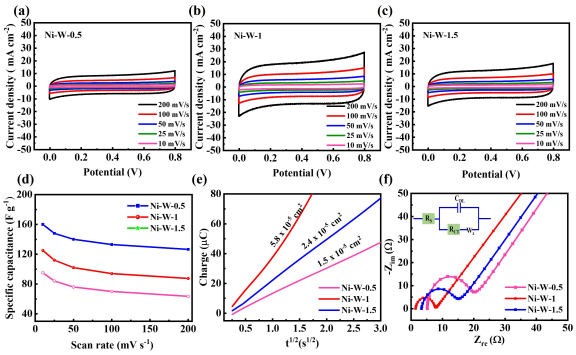

FIGURE 2. (a-c) CV results, (d) corresponding specific capacitance, (e) electrochemical surface area measurements, and (f) EIS results of the samples in a three-electrode system with 6.0 M KOH electrolyte.

mV s^{-1}, respectively. The specific capacitance resulting from the difference in scan rate is shown in Figure 2(d). Ni-W-1 has a high capacitance and a low charge transfer resistance, which indicates a large surface area.

The electrochemically active surface area was determined using chronocoulometric (CC) measurements, as depicted in Figure 2(e). In this graph, the slope directly correlates with the active surface area [7,11,19]. Ni-W-0.5, Ni-W-1, and Ni-W-1.5 surface areas were 1.5 x 10^{-5}, 5.8 x 10^{-5}, 5.2 x 10^{-5}, and 2.4 x 10^{-5} cm^2, respectively. The Ni-W-1 sample has the largest surface area when compared to the others and the Ni-W-1 sample is expected to have a higher electrochemical energy storage capability than the others due to its large surface area, which is a key characteristic of supercapacitors. Internal resistance (R_s) and charge transfer resistance (R_{CT}), could be evaluated using Z-fitting software based on the equivalent Randle circuit, as described elsewhere [11,20]. As

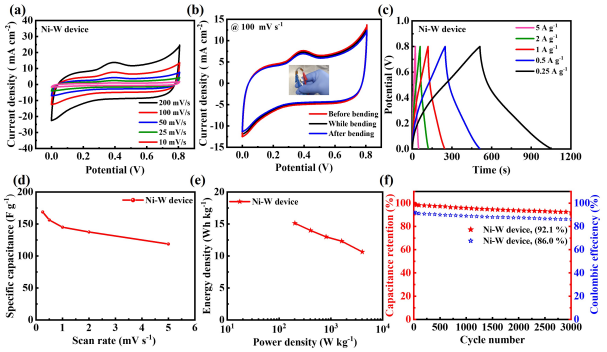

FIGURE 3. (a) CV results, (b) under different bending conditions, (c) GCD curves, (d) specific capacitance, (e) Ragone plot, and (f) capacitance retention and coulombic efficiency of supercapacitor device in the two-electrode system with PVA/KOH gel electrolyte.

can be seen in Figure 2(f), internal resistance and charge transfer resistance were calculated to be 5 and 18.9 Ohm for Ni-W-0.5, 1.3 and 6.8 Ohm for Ni-W-1, 3.2 and 14.5 Ohm for Ni-W-1.5, respectively. It was observed that Ni-W-1 has the lowest internal and charge transfer resistance, implying that it will provide better specific capacitance and expected power density.

The symmetric flexible supercapacitor device, in a two-electrode system, was investigated with the PVA/KOH gel electrolyte [21,22], and Figure 3 displays the results of the electrochemical performance of the flexible supercapacitors.As can be seen in Figure 3(a), the CV results of the Ni-W device at the various scan rates from 25 to 200 mV s^{-1} show a tilted quasi-rectangular shape under the potential window from 0 to 0.8 V. To examine the flexibility and mechanical stability of the solid-state supercapacitor, the CV measurements were carried out under three different bending conditions (before bending, under the bending, and after bending) at the scan rate of 100 mV s^{-1}, resulting that almost no change of the CV results was obtained (Figure 3(b)). The GCPL results of the Ni-W device are also shown in Figure 3(c), and the obtained specific capacitance, calculated by using equation (2), was 144 F g^{-1} at 1 A g^{-1}. The specific capacitance in relation to the current density was also depicted in Fig. 3(d), and the corresponding Ragone plot (Figure 3(e)) was plotted, by using the above equations (3) and (4). The maximum specific energy of 13.3 Wh kg^{-1} with the corresponding specific power of 802 W kg^{-1} at the current density of 1 A g^{-1} was obtained [23,24]. The resultant capacitance retention and coulombic efficiency of the Ni-W device were calculated by using equation (5) and presented in Figure 3(f), resulting in the capacitance retention of 92.1 % and the coulombic efficiency of 86.0 % obtained after 3,000 cycles, resulting in the device's reliable and stable after

the 3,000 cycles.

4. CONCLUSION

A simple and easy hydrothermal synthesis was used to synthesize nickel-doped hexagonal pyramid-like tungsten disulfide (WS_2) for electrode materials in supercapacitor applications. The optimal quantity of nickel doping to WS_2 enhances surface area, charge transfer rate, and capacitance. The symmetric supercapacitor device with 4.5 at. % nickel doping has a high specific capacitance of 144 F g^{-1} at a current density of 1 A g^{-1}, an energy density of 13.3 Wh kg^{-1}, and a power density of 802 W kg^{-1}. Finally, after 3,000 cycles, high specific power retention (92.1%) and coulomb efficiency (86.0%) were demonstrated. These findings show that the nickel-doped WS_2 produced might be employed for all-solid-state supercapacitor flexible electrodes.

AUTHOR STATEMENT

Keshab Pandey: Investigation, Data curation, Writing-original draft preparation, Hae Kyung Jeong: Conceptualization, Revising and Editing draft, Supervision

EDITORS' NOTE

This manuscript was submitted to the Association of Nepali Physicists in America (ANPA) Conference 2023 for publication in the special issue of Journal of Nepal Physical Society.

REFERENCES

1. A. D. Adhikari, S. Singh, and I. Lahiri, "WS_2 @ppy heterostructured high performance supercapacitor self-powered by pvdf piezoelectric separator," J. Alloys Compd. **939**, 168713 (2023).
2. Z. Zhu, Z. Zhang, Q. Zhuang, F. Gao, and et al., "Growth of $mnco_2o_4$ hollow nano-spheres on activated carbon cloth for flexible asymmetric supercapacitors," J. Power Sources **492**, 229669 (2021).
3. M. Fu, R. Lv, Y. Lei, and M. Terrones, "Ultralight flexible electrodes of nitrogen-doped carbon microtube sponges for high performance supercapacitors," Small **17**, 2004827 (2020).
4. T. Mukhiya, B. Dahal, G. Ojha, D. Kang, T. Kim, and et al., "Engineering nanohaired 3D cobalt hydroxide wheels in electrospun carbon nanofibers for high-performance supercapacitors," Chem. Eng. J. **361**, 1225–1234 (2019).
5. K. Pandey and H. K. Jeong, "Ambient plasma treated tungsten disulfide for electrochemical energy applications," J. Phys. Chem. Solids **181**, 111520 (2023).
6. G. P. Ojha, B. Pant, J. Acharya, P. C. Lohani, and M. Park, "Solvothermal-localized selenylation transformation of cobalt nickel mofs templated heterointerfaces enriched monoclinic Co_3Se_4/$CoNi_2Se_4$@activated knitted carbon cloth for flexible and bi-axial stretchable supercapacitors," Chem. Eng, J., **464**, 142621 (2023).
7. G. Ghanashyam and H. K. Jeong, "Plasma treated carbon nanofiber for flexible supercapacitors," J. Energy Storage **40**, 102806 (2021).
8. N. Kamboj, T. Purkait, M. Das, S. Sarkar, and et al., "Ultralong cycle life and outstanding capacitive performance of a 10.8 v metal free micro-supercapacitor with highly conducting and robust laser-irradiated graphene for an integrated storage device, energy," Environ. Sci., **12**, 2507–2517 (2019).
9. V. V. Mohan, M. Manuraj, P. M. Anjana, and R. B. Rakhi, "WS_2 nanoflowers as efficient electrode materials for supercapacitors," Energy Technol., **10**, 2100976 (2022).
10. T. Kajana, A. Pirashanthan, D. Velauthapillai, A. Yuvapragasam, and et al., "Potential transition and post-transition metal sulfides as efficient electrodes for energy storage applications: review," RSC Adv., **12**, 18041–18062 (2022).
11. K. Pandey and H. K. Jeong, "Synthesis of tungsten disulfide for electrochemical energy applications," Mater. Sci. Eng. B **295**, 116601 (2023).
12. C. An, Y. Zhang, H. Guo, and Y. Wang, "Metal oxide-based supercapacitors: progress and prospectives," Nanoscale Adv., **1**, 4644–4658 (2019).
13. Y. Zhong, X. Xia, F. Shi, J. Zhan, and et al., "Transition metal carbides and nitrides in energy storage and conversion," Adv. Sci., **3**, 1500286 (2016).
14. S. Tanwar, A. Arya, A. Gaur, and A. L. Sharma, "Transition metal dichalcogenide (Tmds) electrodes for supercapacitors: a comprehensive review," J. Phys.: Condens. Matter **33**, 303002 (2021).
15. M. Luo, S. Y. Hao, and Y. T. Ling, "Ab initio study of electronic and magnetic properties in ni-doped ws_2 monolayer," AIP ADVANCES **6**, 085112 (2016).
16. S. R. Kadam, R. B. Ziv, and M. B.-Sadan, "A cobalt-doped wS_2/wO3 nanocomposite electrocatalyst for the hydrogen evolution reaction in acidic and alkaline media," New J. Chem., **46**, 20102–20107 (2022).
17. A. S. Rasappan, V. Thangamuthu, M. Natarajan, and D. Velauthapillai, "Kirkendall effect induced nife: WS_2 core-shell nanocubes for dye-sensitized solar cella and battery-type supercapacitor applications," J. Energy Storage, **63**, 106964 (2023).
18. T. Kawai, M. Nakazono, R. Sugimoto, and K. Yoshino, "Change in crystal structure of poly(3-alkylthiophene) upon doping," Synth. Met., **55**, 353–358 (1993).
19. K. Pandey and H. K. Jeong, "Synthesis of tungsten disulfide for electrocatalysts," New Phys.: Saemulli **73**, 403–412 (2023).
20. G. S. Gudavalli, J. N. Turner, and T. P. Dhakal, "Chemical vapor-deposited carbon nanotubes as electrode material for supercapacitor applications," MRS Advances **2**, 3263–3269 (2017).
21. R. K. Sankaralingam, S. Seshadri, J. Sunarso, A. I. Bhatt, and A. Kapoor, "PVA-based KOH polymer gel electrolyte as a membrane separator for zinc-air flow battery, materials," Mater. Today: Proc., **64**, 1649–1654 (2022).
22. H. U.-Rehman, A. Shuja, M. Ali, A. S. Khan, and et al., "Investigation of charge and current dynamics in PVA-KOH gel electrolyte-based supercapacitor," J. Mater. Sci.: Mater. Electron **33**, 2322–2335 (2022).
23. K. Pandey and H. K. Jeong, "Silicon-carbon nanofiber composite film for supercapacitor applications," Chem. Phys. Lett. **834**, 140972 (2024).
24. S. Hussain, I. Rabani, D. Vikraman, A. Feroze, and et al., "One-pot synthesis of W_2C/WS_2 hybrid nanostructures for improved hydrogen evolution reactions and supercapacitors," Nanomaterials **10**, 1597 (2020).